Hygroscopicity of Nitrogen Containing Organic Carbon Compounds: o-aminophenol and p-aminophenol

SCHOLARONE™
Manuscripts

1
2
3 **Environmental Significance Statement**

4

5 3 A wide variety of organic aerosols are emitted to the atmosphere but their influence on

6 4 the climate remains uncertain partly due to aerosol-cloud interactions. Hence,

7 5 understanding the cloud condensation nuclei efficiencies of various organic aerosols is

8 6 needed to improve climate change predictions. Here, the water uptake of two nitrogen-

9 7 containing organic aerosols, *o*-aminophenol and *p*-aminophenol were investigated under

10 8 subsaturated and supersaturated conditions for the first time. Our results show that both

11 9 isomeric compounds exhibit size-dependent hygroscopic growth in the same range of

12 10 dominant organics in aerosols, with *o*-aminophenol more so than *p*-aminophenol. Our

13 11 results highlight that a small variation in the position of functional groups can have a major

14 12 influence in the water uptake mechanism and changes to particle morphology. This

15 13 finding adds a new dimension to the growing body of knowledge that emphasizes the role

16 14 of physiochemical properties of organic compounds such as size, morphology, chemical

17 15 structure, and solubility in driving aerosol water uptake. Hence, these properties must be

18 16 accounted for when predicting the impact of organic aerosols on the climate.

19 17

Hygroscopicity of Nitrogen Containing Organic Carbon Compounds: *o*-aminophenol and *p*-aminophenol

Kotiba A. Malek[1], Dewansh Rastogi[1], Hind A. Al-Abadleh[2], and Akua A. Asa-Awuku[1,3]

[1]Department of Chemical and Biomolecular Engineering, University of Maryland, College Park, MD 20742, United States

[2]Department of Chemistry and Biochemistry, Wilfrid Laurier University, Waterloo, ON N2L 3C5, Canada

[3]Department of Chemistry and Biochemistry, University of Maryland, College Park, MD 20742, United States

Correspondence to: Akua Asa-Awuku (asaawuku@umd.edu) and Hind A. Al-Abadleh (halabadleh@wlu.ca)

Abstract

Nitrogen-containing Organic Carbon (NOC) is a major constituent of atmospheric aerosols and they have received significant attention in the atmospheric science community. While extensive research and advancements have been made regarding their emission sources, concentrations, and their secondary formation in the atmosphere, little is known about their water uptake efficiencies and their subsequent role on climate, air quality, and visibility. In this study, we investigated the water uptake of two sparingly soluble aromatic NOC: o-aminophenol (oAP) and p-aminophenol (pAP) under subsaturated and supersaturated environments using Hygroscopicity Tandem Differential Mobility Analyzer (H-TDMA) and a Cloud Condensation Nuclei Counter (CCNC), respectively. Our results show that oAP and pAP are slightly hygroscopic with comparable hygroscopicities to various studied organic aerosols. The supersaturated single hygroscopicity parameter (κ_{CCN}) was measured and reported to be 0.18±0.05 for oAP and 0.04±0.02 for pAP, indicating that oAP is more hygroscopic than pAP despite them having the same molecular formulae. The observed disparity in hygroscopicity is attributed to the difference in functional group locations, interactions with gas phase water molecules, and the reported bulk water solubilities of the NOC. Under subsaturated condition, both oAP and pAP aerosols showed size dependent water uptake. Both species demonstrated growth at smaller dry particle sizes, and shrinkage at larger dry particle sizes. The measured Growth Factor (G_f) range, at RH = 85%, for oAP was 1.60-0.74 and for pAP was 1.53-0.74 with increasing particle size. The growth and shrinkage dichotomy is attributed to morphological particle differences verified by TEM images of small and large particles. Subsequently, aerosol physicochemical properties must be considered to properly predict the droplet growth of NOC aerosols in the atmosphere.

Introduction

Aerosol particles have major implications on global climate, air quality, and human health. Aerosols can be emitted from a variety of sources (e.g., biomass burning, sea spray, combustion processes, desert dust, and volcanic eruptions)[1–3] or they can be generated in the atmosphere through various chemical processes (e.g., nucleation, condensation, and oxidation).[4–6] Once suspended in the atmosphere, aerosols can influence Earth's radiative budget through their direct and indirect interaction with solar radiation.[2,4,7–9] The direct effect is based on the aerosol's ability to directly scatter and absorb solar radiation. As for the indirect effect, aerosol particles can act either act as cloud condensation nuclei (CCN)—taking up water vapor and forming clouds in the process[4,7,10] or as ice nucleating particles to form ice clouds.[11] Hence, aerosols' CCN efficiencies to uptake water (hygroscopicity) can directly affect the amount of cloud's light absorption or scattering that takes place. The latest Intergovernmental Panel on Climate Change (IPCC) estimate of climate radiative forcing from the aerosol/cloud interaction is -0.7 Wm^{-2} (uncertainty range -1.8 to -0.3 Wm^{-2}).[12] The large uncertainty associated with aerosol-cloud interactions highlights the complexity associated with aerosols and their effect on cloud formation. While aerosol particles are composed of organic and inorganic species, the primary source of uncertainty stems from abundant and poorly understood organic aerosols.[13,14]

Organic aerosols (OA) are ubiquitous in the atmosphere and account for a large fraction of atmospheric aerosols.[13,15] Within the last decade, the atmospheric chemistry field has made substantial advances in aerosol speciation, chemical compositions of OA, and the chemical processes that OA undergo in the atmosphere. These advances were

highlighted in published reviews that include but not limited to Erven et al.[6]; Hallquist et al.[16]; Kanakidou et al.[13]; Kroll and Seinfeld[17]; and Mahilang et al.[18] Despite these advances. the uncertainty in the hygroscopic-related properties of atmospheric OA remains large.[15]

Nitrogen-containing organic carbon (NOC) are a major class of OA growing in importance due to a decline in regional sulfates and their prominent presence within atmospheric aerosols.[15,19–23]. Wedyan *et al.* (2007)[21] discovered that 80% of nitrogen over the coastal Gulf of Aqaba was attributed to NOC.[21] Another study *by* Cornell *et al.*[24] investigated the atmospheric chemical composition in Oahu, Hawaii, and found that approximately 30% of the total nitrogen was stored in NOC form.[24] The abundance of NOC in the atmosphere is attributed to the wide range of primary and secondary emission sources.[25] Primary sources such as biomass burning and both anthropogenic and biogenic sources, are responsible for approximately 27.4 Tg of NOC annually.[13] As for secondary sources, the formation of NOC within the atmosphere remains unexplored. Various studies have shown that NOC can be formed in the atmosphere from chemical processes involving secondary organic aerosol (SOA) (e.g., but not limited to Darer et al.[26]; Liu et al.[27]; Vidović et al.[28]; Zhang et al.[29]). For instance, a wide range of NOC species can be formed from the ozonolysis of *α*-pinene and *m*-xylene in the presence of ammonia.[27] Another study found that the atmospheric presence of NOC is attributed to the reaction of ammonium with oxidized organics (e.g., formate, acetate, pyruvate, malonate).[29]

To further enhance our knowledge of NOC and their role within atmospheric chemistry and climate impacts, investigating the physiochemical properties of NOC

4

aerosols is necessary.[7] One vital physicochemical property is hygroscopicity, which describes the water uptake ability of aerosols under subsaturated and supersaturated conditions.[30] While extensive efforts have been allocated to investigate and report the water uptake behavior of atmospherically relevant OA compounds, further research remains needed. This is due to the presence of a wide range of OA in the atmosphere making quantifying their hygroscopic properties a formidable task. To circumvent this challenge, theoretical models have been used to predict the hygroscopicity of OA, which are semi-empirical and often rely on parametrization of water solubility and extrapolation from lab measurements of one class of OA to another.[31] Such simplistic approach fails to accurately capture the non-ideal behavior that is developed from solubility,[32] liquid-liquid phase separation,[33,34] surface partitioning,[35] and morphology.[36] Also, these limitations highlight the fundamental importance to investigate the hygroscopicity of different classes of OA through laboratory measurement techniques. As such, various studies have undertaken a systematic approach by investigating the hygroscopicity of OA through the lens of other physicochemical properties such as functional groups, molecular weight, and bulk water solubility.[37–42] For example, Suda *et al.*[42] investigated the CCN activity of OA possessing different functional groups and reported a direct influence of functional group on water uptake. Specifically, it was reported that the hygroscopicity of an organic compound with hydroxyl or carboxyl groups is higher than that with nitrate or methylene groups.[42] Other studies investigated a family of organic compounds, such as carboxylic acids[37,43] or amino acids.[37,44] The water uptake of amino acids has been reported due to their important involvement in the nitrogen cycle in the atmosphere (e.g., but not limited to Chan et al.[45]; Han et al.[43]; Luo et al.[44]; Marsh et al.[37]). Luo *et al.*[44]

investigated the water uptake using a hygroscopicity tandem differential mobility analyzer (H-TDMA) system, under a range of relative humidity (RH), of a series of amino acids, including aspartic acid, glutamine, and serine along with their mixtures with ammonium sulfate. The results of Luo *et al.*[44] show that bulk water solubility play a major role in understanding the hygroscopicity of these amino acids, and that the presence of ammonium sulfate influence the phase state and hygroscopicity of the mixture.[44]

To contribute to the mechanistic understanding of OA hygroscopicity, we explored two NOC aminophenol isomers: *o*-aminophenol (*oAP*) and *p*-aminophenol (*pAP*). [46,47] To our knowledge, no previous literature has reported on the hygroscopicity of pure aromatic compounds that contain nitrogen. Previous studies have employed other aromatic compounds to produce secondary organic aerosols (SOA) of mixed chemical composition. For example, the study by *Hilderbrandt Ruiz et al.*[48] involved measuring the water uptake of SOA produced from the photooxidation of toluene. Another study by *Nakao et al.*[49] investigated the SOA formation from benzene, toluene, *m*-xylene using an environmental chamber under different conditions. Similarly, various studies have investigated the water uptake of SOA formed from monoterpenes ($C_{10}H_{16}$) such as *α*-pinene, *β*-pinene, limonene, and terpinene (Huff Hartz et al.[50]; Prenni et al.[39]; Duplissy et al.[51]; Frosch et al.[52], to name a few). Additionally, while previous studies have reported the hygroscopicity of SOA from aliphatic amines,[53] no previous study has explored aromatic amines, whether in single- or multi-component systems.

Exploring single component composition instead of a mixture of components offer valuable knowledge with respect to how various physicochemical properties such as solubility, O:C ratio, functional groups, chemical composition, and structure impact water

uptake in aerosol particles. This is highlighted by the previously published CCN work that have investigated single component aerosols (e.g., but not limited to Marsh et al.[37]; Peng et al.[54]; Raymond et al.[55]; Han et al.[43]; Dawson et al.[56]; Estillore et al.[57]). Therefore, our study aims to enhance our understanding of the physiochemical properties effecting water uptake. The ring structure of oAP and pAP will provide us with a new perspective on the effect of aromaticity. Additionally, the two functional groups ($-NH_2$ and $-OH$) on the aromatic ring in oAP and pAP add to the growing database of hygroscopicity of OA with different functional groups. Previous studies have invested in understanding the hygroscopic properties of OA with different functional groups (Han et al.[43]; Petters et al.[58]; Suda et al.[42], to name a few); however, no previous reports were conducted on compounds containing $-NH_2$ and $-OH$ together. Finally, oAP and pAP enable us to explore the effect of solubility on hygroscopicity while maintaining the same O:C ratio, chemical composition, and functional groups.
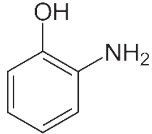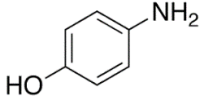
The objective of this paper is to investigate the water uptake of oAP and pAP under subsaturated condition using a Hygroscopicity Tandem Differential Mobility Analyzer (H-TDMA) and supersaturated condition using a Cloud Condensation Nuclei Counter (CCNC). Results were analyzed through the lens of solubility and morphological properties and highlight the importance of physicochemical properties on the water uptake of NOC compounds.. Hence, understanding the water uptake of these aminophenol compounds will add a new dimension to the growing knowledge on the impact of functional groups on hygroscopicity.

Experimental and Data Analysis

Chemicals. *o*-aminophenol (99%, CAS: 95-55-6, Sigma-Aldrich) and *p*-aminophenol

(≥98%, CAS: 123-30-8, Sigma-Aldrich) were used in this study. All chemicals were used

as received without further purification. The chemical structures and physical properties

of both chemicals are summarized in **Table 1**.

Table 1. The chemical structures and the relevant properties of *o*-aminophenol and *p*-aminophenol

Chemical	Abbv.	Structure	Molecular Weight [g mol^{-1}]	Density [g mL^{-1}]	Bulk Solubility, S_{bulk} (in H_2O) [g L^{-1}]
o-aminophenol	*oAP*		109.13[a]	1.33 [a]	19.6[c]
p-aminophenol	*pAP*		109.13[b]	1.13 [b]	15.7[c]

[a] *National Center for Biotechnology Information (2022). PubChem Compound Summary for CID 5801, 2-Aminophenol. Retrieved April 3, 2022 from https://pubchem.ncbi.nlm.nih.gov/compound/2-Aminophenol.*
[b] *National Center for Biotechnology Information (2022). PubChem Compound Summary for CID 403, 4-Aminophenol. Retrieved April 3, 2022 from https://pubchem.ncbi.nlm.nih.gov/compound/4-Aminophenol*
[c] *Rumble, J. R.; Lide, D. R.; Bruno, T. J. CRC handbook of chemistry and physics: a ready-reference book of chemical and physical data, 2017*

Aerosol Generation. A 0.1 g L^{-1} solution was prepared for each chemical using ultra-

purified water (18 MΩ cm^{-1}, Millipore). The prepared solutions were sonicated to ensure

dissolution prior to atomization. The aerosols were then generated using a constant

output Collison Nebulizer (Atomizer; TSI 3076). The aerosols generation method has

been used and described in previous CCN literature.[43,55,57,59,60]

The wet aerosols were dried (< 5% RH) using silica gel dryers. The water uptake of the

generated dry aerosols was then measured with two different experimental setups; a) H-

TDMA (subsaturated conditions) and b) CCNC (supersaturated conditions) (**Figure 1**). In

addition, TEM images were obtained using a sample collection setup shown in **Figure 1**.
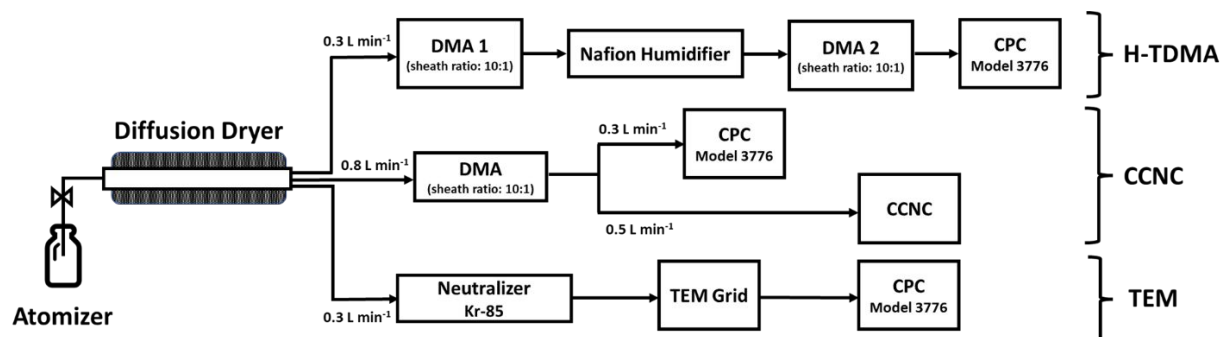

Figure 1. The experimental setup for subsaturated H-TDMA measurements, supersaturated CCNC measurements, and TEM sample collection. Abbreviations are: DMA: Differential Mobility Analyzer, CPC: Condensation Particle Counter, CCNC: Cloud Condensation Nuclei Counter, and TEM: Transmission Electron Microscope.

Hygroscopicity Tandem Differential Mobility Analysis. The water uptake of *oAP* and *pAP* was evaluated under subsaturated conditions using the widely employed H-TDMA. The operation of the H-TDMA has been described in detail in previous literature.[61,62] An overview of the H-TDMA experimental setup is shown in **Figure 1**. The dry aerosols, generated from a 0.1 g L^{-1} solution, were size selected (30-200 nm) by an electrostatic classifier (DMA 1, TSI 3082; flow rate = 0.3 L min^{-1}). The size-selected particles were then humidified to RH = 85% ± 5% using a nafion humidification line (PermaPure M.H. series). The size distribution of the wet aerosol particles was then scanned using a second electrostatic classifier (DMA 2, TSI 3085; flowrate 0.3 L min^{-1}), and the concentrations were measured using a Condensation Particle Counter (CPC; TSI 3776; flow rate = 0.3

L min^{-1}). The Growth Factor (G_f) is the ratio between the wet mobility diameter (D_{wet}) and the dry mobility diameter (D_{dry}) (**Eq. 1**). G_f was calculated for each size-selected dry mobility diameter, averaged, and reported with its respective standard deviation.

$$G_f = \frac{D_{wet}}{D_{dry}} \tag{1}$$

The RH of the H-TDMA setup was calibrated with inorganic ammonium sulfate (*see Supplemental Information*; Taylor *et al.*[63]).

Cloud Condensation Nuclei Analysis. The water uptake of *oAP* and *pAP* was tested under four different supersaturations (0.46, 0.67, 0.86, and 1.08%), that represent warm clouds, using a commercially available Cloud Condensation Nuclei Counter (CCNC; Droplet Measurement Technologies). The operation of the CCNC has been extensively described in previous literature.[64–66] An overview of the CCNC experimental setup is shown in **Figure 1**. A flow stream (flow rate = 0.8 L min^{-1}) of dried aerosol particles were charged in a Kr-85 bipolar neutralizer to produce an equilibrium distribution of electrically charged particles.[67] The charged particles were then passed to a DMA (TSI 3080) in scanning mode and a size distribution from 8 to 352 nm was measured every 2.25 minutes. Downstream from the DMA, the aerosol stream was bifurcated with one stream (flow rate = 0.3 L min^{-1}) flowing into a CPC (TSI 3776) where the particle concentration (CN) was measured, while the other stream (flow rate = 0.5 L min^{-1}) flowing into the CCNC where the activated particle concentration (CCN) was measured. The activated fraction is the ratio between CCN and CN and was measured at four different supersaturations, and the critical diameter (D_d), defined as the dry particle diameter size at which 50% of

10

the particles form droplets, was calculated with Scanning Mobility CCN Analysis (SMCA).[66] The SMCA applies a charge correction followed by fitting a sigmoid curve through the activated fraction to obtain the D_d.[66,67] At each supersaturation, 10 critical diameters were obtained for each chemical, and were used to calculate the hygroscopicity. To determine the CCNC's supersaturations, a widely used calibration procedure was conducted with inorganic ammonium sulfate.[55,56,68–71] Ammonium sulfate has been used in various literature for CCNC calibration for hygroscopicity measurements of organic aerosol.[55,56,69–71] The calibration was conducted prior to the experiments, and the calibrated supersaturations are reported in the *Supplemental Information*.

Water vapor condensation on aerosol particles and droplet growth can be thermodynamically described by Köhler theory. The theory is based on equilibrium thermodynamics and describes the vapor pressure and saturation, *S*, as follows:[72]

$$S = a_w exp\left(\frac{4\sigma_{s/a} M_w}{RT\rho_w D_{wet}}\right) \tag{2}$$

where a_w represents the water activity coefficient, $\sigma_{s/a}$ is the surface tension of the droplet, R is the universal gas constant, T is the sample temperature, D_{wet} is diameter of the wet droplet, and ρ_w and M_w are the density and molecular weight of water, respectively.[72]

Based on the Köhler theory, the hygroscopicity of aerosol particles can be expressed in terms of a single hygroscopicity parameter, κ, assuming the solute to be sufficiently dilute (i.e., ideal solubility).[30] Hence, supersaturated κ-hygroscopicity (κ_{CCN}) of *oAP* and *pAP* can be expressed using the following equation:[30]

11

$$\kappa_{CCN} = \frac{4\left(\dfrac{4\sigma_{s/a}\,M_w}{RT\rho_w}\right)^3}{27D_d{}^3 ln^2 s_c} \qquad (3)$$

where D_d is the critical activation diameter and s_c is the CCNC instrument supersaturation.

The κ_{CCN} derived from the equation above is assumed to be constant as s_c is directly

proportional to $D_d^{-1.5}$.[30]

Transmission Electron Microscopy (TEM). The morphology of nano-sized aerosol

particles of *o*AP and *p*AP were measured using a Transmission Electron Microscopy

(JEOL 2100 TEM; LaB$_6$ filament)—a method previously described in literature.[34,73] An

overview of the TEM sample collection is presented in **Figure 1**. In brief, the generated

dry aerosol stream (0.3 L min^{-1}) was charged with a neutralizer (Kr-85, TSI 3077A). The

charged particles were then deposited for 4 hours onto an electrically grounded lacey

carbon-coated copper TEM grid (TED PELLA). The deposited particles were then imaged

at an accelerating voltage of 200 kV and a magnification range of 50-150 k. To minimize

sample damage, the exposure time was limited to 90 sec.

Results and Discussion

Hygroscopicity under supersaturated conditions

The κ-values for *o*AP and *p*AP are reported and compared to other atmospherically

relevant pure organic compounds (obtained from literature; refer to Table 2).. To

understand the hygroscopicity of *o*AP and *p*AP aerosols under supersaturated conditions,

10 critical diameters (D_d) were measured at four different supersaturations (0.46, 0.67,

0.86, and 1.08%) and the average κ_{CCN} for each compound was calculated according to

Eq. 3. Both *oAP* and *pAP* were observed to be slightly hygroscopic, under supersaturated conditions, with κ-values between 0.04-0.18. The average κ_{CCN} for *oAP* and *pAP* aerosols were 0.18±0.05 and 0.04±0.02, respectively. These values are consistent with κ-values, obtained from various studied organic compounds, of less than 0.4,[37,43,74] specifically, κ-values of different carboxylic acids, amino acids, sugars, and cycloalkenes as listed in **Table 2** and **Figure 2a**. Hence, it is evident that the water uptake of both *oAP* and *pAP* falls within the range of hygroscopicity of other atmospherically significant functional groups suggesting that the presence of both functional groups (–OH and –NH$_2$) in aminophenols results in an average water uptake behavior similar to that of other functional groups.
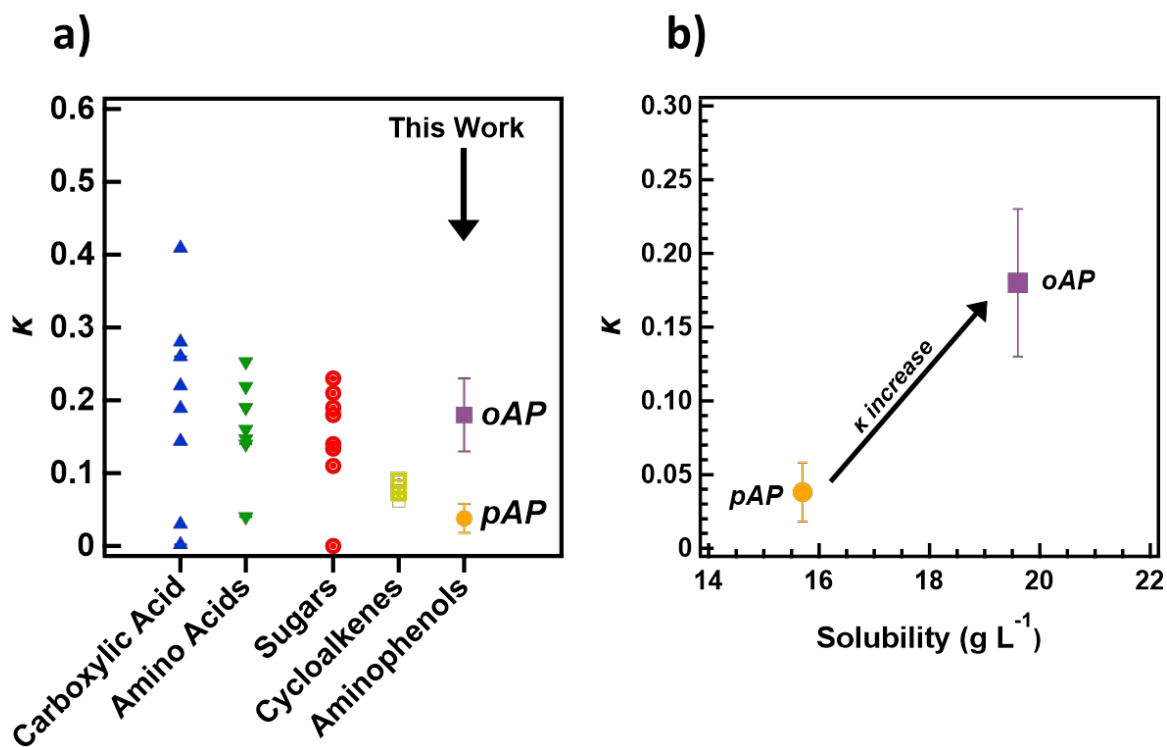

Figure 2. a) Hygroscopicity of organic aerosol reported in literature and compared to the aminophenols studied here, *oAP* and *pAP*. A detailed summary of the chemicals, κ-

13

values, and their respective references is found in **Table 2**. b) The relationship between

hygroscopicity and bulk water solubility for *oAP* and *pAP* at 25 °C. Error bars for *oAP* and

pAP represent standard deviation of 40 repeated measurements.

Table 2. Summary of literature κ-hygroscopicity of various organic compounds of atmospheric relevance

Organic Groups	Compounds	κ	References
Carboxylic Acid	Malonic Acid	0.26	*Han et al.*[43]
	Succinic Acid	0.002	*Peng et al.*[54]
	Pimelic Acid	0.03	*Han et al.*[43]
	Maleic Acid	0.28	*Choi and Chan*[75]
	Tartaric Acid	0.22	*Han et al.*[43]
	Citric Acid	0.19	*Marsh et al.*[37]
	Glutaric Acid	0.14	*Marsh et al.*[37]
	Oxalic Acid	0.41	*Marsh et al.*[37]
Amino Acids	Glycine	0.04	*Han et al.*[43]
	L-Aspartic	0.14	*Han et al.*[43]
	L-Glutamine	0.16	*Han et al.*[43]
	Serine	0.19	*Han et al.*[43]
	L-Arginine	0.147	*Marsh et al.*[37]
	L-Lysine	0.219	*Marsh et al.*[37]
	L-Valine	0.253	*Marsh et al.*[37]
Sugars	Fructose	0.23	*Han et al.*[43]
	Sucrose	0.10	*Dawson et al.*[56]
	Mannose	0.14	*Han et al.*[43]
	L-Arabitol	0.19	*Han et al.*[43]
	D-Mannitol	-0.01	*Han et al.*[43]
	Galactose	0.134	*Marsh et al.*[43]
	Xylitol	0.18	*Bilde et al.*[76]
Cycloalkenes	Cyclopentene	0.09[a]	*Varutbangkul et al.*[77]
	Cyclohexene	0.073[a]	*Varutbangkul et al.*[77]
	Cycloheptene	0.071[a]	*Varutbangkul et al.*[77]
	Cyclooctene	0.062[a]	*Varutbangkul et al.*[77]

[a] *κ-value was calculated* [78] *from G_f reported by Varutabangkul et al.*[77]

Previous studies by Bilde et al.[79]; Chen at al.[80]; Han et al.[43]; Suda et al.[42,81] to name a few reported variation in OA hygroscopicities with organic functionality. For example, Han *et al.*[43] showed a quantitative increase in κ-values based on functional groups in the order of (–COOH or C=O) > (–OH) > (–CH_3 or –NH_2).[43] Another study by Suda *et al.*[81] examined the hygroscopicity of various SOA under subsaturated environments, and reported a relationship between κ-hygroscopicity and polarity in organic compounds, with highly polar SOA being more hygroscopic. [81] The conclusions of these studies suggest that other physiochemical properties contribute, along with the type of functional groups, to the hygroscopicity of organic compounds.

To highlight the significance of other physicochemical properties (specifically solubility), **Figure 2b** shows a significant difference in κ-values between *oAP* and *pAP*. Despite having the same molecular formulae and type of functional groups, *oAP* (κ_{CCN} = 0.18±0.05) is more hygroscopic than *pAP* (κ_{CCN} = 0.04±0.02). This difference in κ_{CCN} *(i.e.,* hygroscopicity) is attributed to the difference in bulk water solubility between *oAP* and *pAP*. Previous studies have concluded that the bulk water solubility range of 0.1–100 g L^{-1} determines the CCN activity of organic compounds.[41,82–84] The bulk water solubility of both *oAP* and *pAP* falls in the range of slightly soluble compounds with values of 19.6 g L^{-1} and 15.7 g L^{-1}, respectively. Under subsaturated hygroscopic conditions, compounds with limited solubility are composed of an insoluble core surrounded by a saturated solution.[43] Hence, *oAP* having the higher solubility, has a greater molar concentration in the saturated solution, leading to *oAP* being more hygroscopic than *pAP*. This increase in hygroscopicity based on water solubility has been observed in various OA such as, glyoxylic acid and 4-methylphthalic acid in Chan et al.[40]; maleic acid and molonic acid in

Han et al.[43]; aspartic acid and azelaic acid in Huff-Hartz et al.[50]; and polycatechol and polyguaiacol in Malek et al.[85], to name a few.

Hygroscopicity under subsaturated conditions

The water uptake of *oAP* and *pAP* under subsaturated conditions was measured and analyzed based on morphological properties. Subsaturated measurements were completed under constant RH (85 ± 5%), and the measured wet mobility diameters and growth factors are shown in **Figure. 3**. For both *oAP* and *pAP* the water uptake was size-dependent highlighting the presence of two distinct regions referred to as Growth and Shrinkage in **Figure 3**. Here, the term 'Growth' refers to G_f values greater than 1, while the term 'Shrinkage' refers to G_f values less than 1. The experimental G_f values for *oAP* and *pAP* inversely correlated with the dry mobility diameter. For *oAP*, the G_f values range between 1.6-0.74 with increasing dry mobility diameter. For dry mobility diameters ≤ 120 nm, *oAP* aerosols were shown to take up water and grow when exposed to humidification. This water uptake behavior is highlighted by the G_f values greater than 1 for dry mobility diameter ≤ 120 nm. *oAP* aerosols shrank for dry mobility diameter ≥ 120 nm where G_f values are less than 1 (**Figure 3a**). Similarly, the G_f values for the *pAP* system follow the same trend as the *oAP* system. The *pAP* G_f values decrease with increasing dry mobility diameter, with G_f values ranging between 1.5-0.74. However, and in contrast to *oAP* aerosols, the *pAP* aerosol shrinks at a smaller dry mobility diameter ≥ 60 nm (**Figure 3b**).
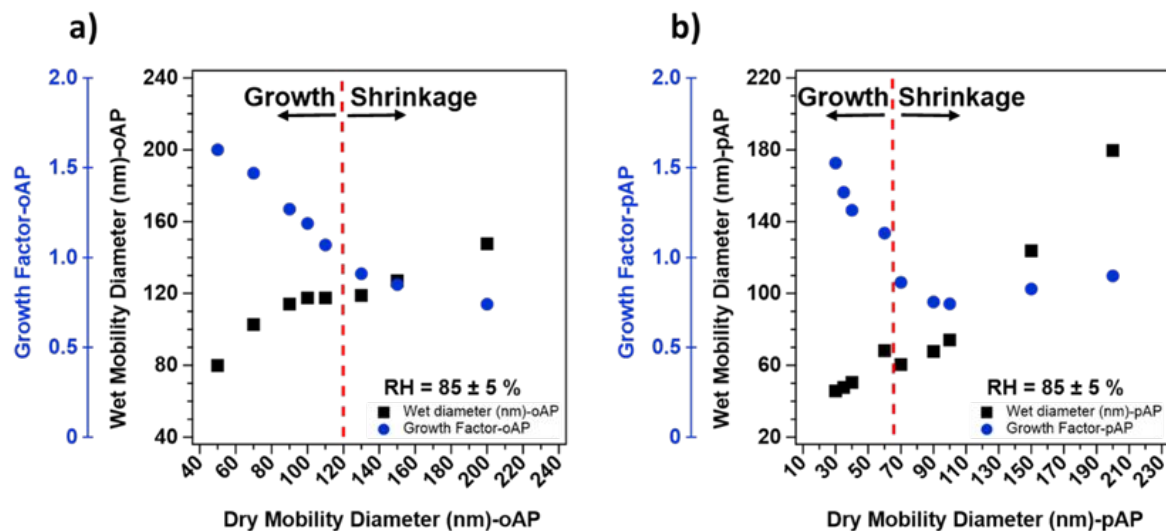
Figure 3. H-TDMA measurements and analysis showing the growth factors versus dry mobility diameters (blue circles) and wet mobility diameters versus dry mobility diameters (black squares) for a) *oAP* and b) *pAP*. Red vertical line indicating the dry mobility diameter where growth to shrinkage transition takes place. Error bars (standard deviation) are included, but small to be visible.

To our knowledge no previous literature has detected a trend similar to our study, where a single component aerosol system undergoes droplet growth and shrinkage across a range of ultrafine dry mobility diameters. Several studies by Cheng et al.[86]; Laskina *et al*.[87]; Mahish and Collins[88] (to name a few) have reported size dependence in the uptake of water of various atmospheric aerosols. However, such observations were made on multicomponent aerosol systems. Laskina *et al*.[87] reported a difference in the water uptake based on particle sizes obtained from a mixture of ammonium sulfate and different OA. This difference was attributed to changes in the mixing state observed for different sized particles.[87] A study by Han *et al*.[43] reported G_f values less than 1 (200 nm; 90% RH) for azelaic and suberic acid using an H-TDMA setup.[43] The shrinking behavior

17

was attributed to morphological limitations of the aerosol particles.[43] Specifically, water adsorption at the surface of the particle could potentially lead to structural rearrangement at the microscale causing particles to collapse and shrink.[36,89,90]

Figure 4 shows representative TEM images for *oAP* and *pAP* in two particle size ranges. The particle morphology is dependent on particle sizes. At small sizes (≤ 50 nm), the shape of the particles appears spherical for both *oAP* and *pAP* aerosols. These small particles are compact, and hence, when water condenses on their surface, they grow in size. Thus, droplet growth and positive G_f are observed for both *oAP* and *pAP* at small dry mobility diameters.
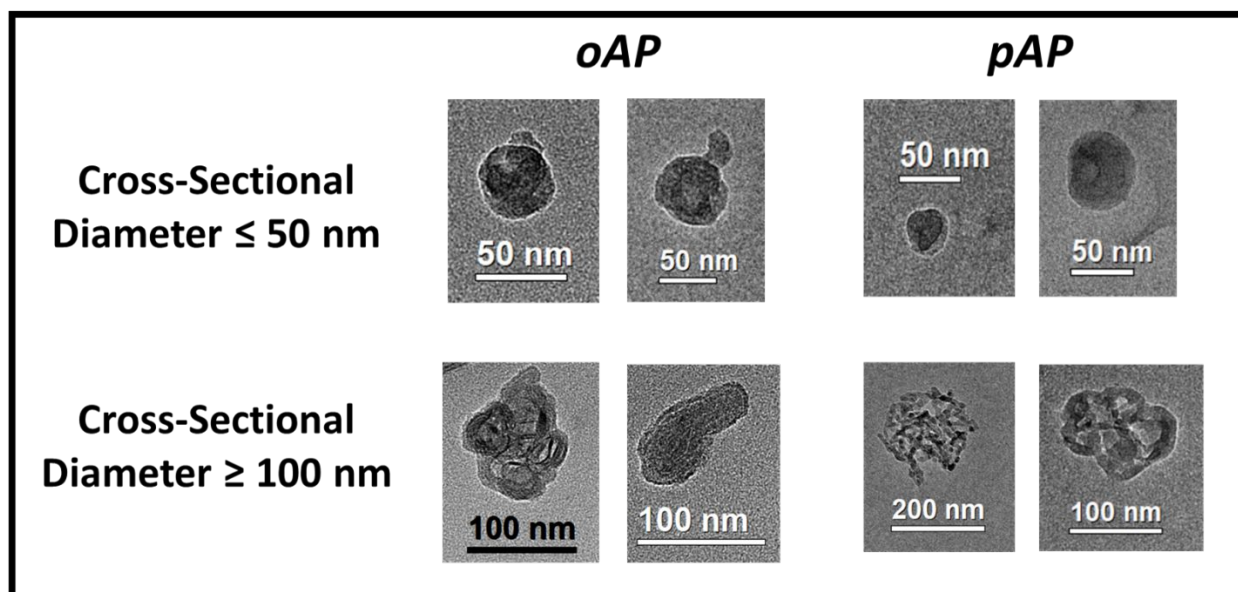

Figure 4. Representative TEM images showing morphological difference between small and large cross-sectional diameter size particles for *oAP* and *pAP*. Sizes within each image represents scale bar. Additional images are provided in **Figures S5** and **S6, S7, and S8** in the *Supporting Information*.

Conversely, large size particles (≥ 100 nm) appear to contain void spaces. They can be formed of smaller elongated subunits. Such morphology at large sizes, makes these subunit particles more susceptible to collapse and rearrangement, as previously postulated by *Mikhailov et al.*.[90] TEM images support the observed shrinking in large *oAP* and *pAP* particles, where G_f = 0.74, and the collapsed particle is reduced in diameter by ~25%. The size-dependent morphology is consistent with the presence of multiple nucleation sites on the surface of aqueous droplets: as the solvent evaporates, it may leave behind structures with void spaces[91,92] , which are more prevalent in the *pAP* dry particle size distribution.

The difference between the water uptake of *oAP* particles at larger sizes (< 120 nm) than *pAP* (< 60 nm) can be attributed to chemical bonding. The functional groups (–OH and –NH_2) in *oAP* can engage in intramolecular hydrogen bonding due to their *ortho*-positioning on the benzene ring. This reduces the number of hydrogen bonds that they can engage in with other neighboring molecules. Hence, *oAP* is less likely to form structures consisting of sub-units compared to *pAP*. As for *pAP*, due to the functional groups being in *para*-position of the benzene ring, hydrogen bonding with other molecules is more likely to occur. In addition, due to the symmetry of the *para*- structure, *pAP* molecules are prone to having a stronger π-π stacking than *oAP*. This is due to the involvement of the electrons, from –OH and –NH_2, in resonance structures causing a high electron density in the benzene ring. Hence, *pAP* particles are more often to consist of sub-units and, as result, more likely to collapse at smaller sizes than *oAP*.

Moreover, the data in **Figure 3** can be used to theoretically estimate the concentration of the aminophenol particles in the droplet at the nanoscale (C_{nano}) from the

value of the wet and dry mobility diameters at $G_f = 1$ assuming spherical particles and using a density of water of 1 g cm^{-3} for comparison with solubility in **Table 1**. **Table 3** lists the parameters used in calculating C_{nano} and the corresponding solute:solvent mass ratio for the particle and bulk systems. This calculation assumes that the mass of *oAP* and *pAP* are fully dissolved in the wet volume. Hence, the C_{nano} calculation can be considered the upper limit of the concentration of a deliquesced aerosol solute.

Table 3: Estimation of particle solubility from hygroscopic growth data in **Figure 3**

o-aminophenol (oAP)							
Wet Diameter	**Wet Volume**	**Dry Diameter**	**Dry Volume**	**Mass of oAP**	**Vol. of H$_2$O** $V_{H2O}(cm^3)^c$	**C$_{nano}$** (g L^{-1})^d	**Solute:solvent mass ratio^e**
D_{wet} (nm)	V_w (cm^3)^a	D_{Dry} (nm)	V_d (cm^3)^a	m (g)^b			
140	1.4×10^{-15}	120	9×10^{-16}	1.2×10^{-15}	5.3×10^{-16}	2264	2.3
p-aminophenol (pAP)							
Wet Diameter	**Wet Volume**	**Dry Diameter**	**Dry Volume**	**Mass of pAP**	**Vol. of H$_2$O**	**C$_{nano}$** (g L^{-1})^d	**Solute:solvent mass ratio^e**
D_{wet} (nm)	V_w (cm^3)^a	D_{Dry} (nm)	V_d (cm^3)^a	m (g)^b	$V_{H2O}(cm^3)^c$		
120	9×10^{-16}	65	1.4×10^{-16}	1.6×10^{-16}	7.6×10^{-16}	211	0.21

Notes: ^{a} volume for spherical particles = $\pi d^3/6$, ^{b} mass = V_d·bulk density (g cm^{-3}). Bulk densities of oAP and pAP are 1.33 and 1.13 g cm^{-3}.[93] ^{c} $V_{H2O} = V_w - V_d$, ^{d} $S_{nano} = m \cdot 1000/V_{H2O}$. ^{e} Mass ratio = $m/(V_{H2O} \cdot 1$ g cm$^{-3})$.

Values of C_{nano} are ~ 120x and 14x higher than the S_{bulk} for *oAP* and *pAP*, respectively. Also, C_{nano} for *oAP* is 11x higher than that of *pAP* whereas S_{bulk} for *oAP* is 1.2x higher than that of *pAP*. This implies that despite *o*AP and *p*AP having a high bulk water solubility, on the nanoscale they are not fully dissolved. The particles are more likely to be composed of an insoluble core that is consistent with partially soluble species.[32,43]

These trends highlight the limitation of using bulk water solubility of organic compounds in Köhler based hygroscopic models of nanosized aerosol particles composed of sparingly soluble organic compounds. Consequently, it also emphasizes the importance of accounting for solubility limits when evaluating hygroscopic properties; molar volume alone is not necessarily a driver for droplet growth; especially in this case where structural isomers are examined. The calculated concentration enhancement is due to the increase in surface area with consequences on dissolution rate.[94,95] Therefore, intermolecular and intramolecular forces need to be taken into account to understand changes to water uptake behavior with size of OA, specifically for isomeric compounds.

Summary and Implications

The hygroscopic properties of two NOC compounds namely, *o*-aminophenol and *p*-aminophenol were investigated under supersaturated and subsaturated conditions. Under supersaturated conditions, the hygroscopicity is reported in terms of the single hygroscopicity parameter (κ). The measured supersaturated hygroscopicity indicates that both *oAP* and *pAP* are slightly hygroscopic with κ-values comparable with other organic compounds of atmospheric-relevance. Under the subsaturated condition of 85 ± 5% RH, the hygroscopicity studies of these two aminophenols reveal that *oAP* is more hygroscopic than *pAP, which* is attributed to *oAP* having a higher bulk water solubility. The growth factor obtained, under subsaturated conditions, is dependent on particle size for both *oAP* and *pAP*. The range of growth factors calculated were 1.6-0.74 (*oAP*) and 1.5-0.74 (for *pAP*) with increasing dry diameter indicating that the particles undergo both growth and shrink depending on size. To explain this contrast in behavior, TEM images for both compounds were collected at small (≤ 50 nm) and large (≥ 100 nm) cross-

sectional diameters sizes. The difference in morphology between small and large particles aided in explaining the growth and shrinkage behavior. Small size particles were spherical in shape, while large size particles contained void spaces and appeared to consist of small sub-particles. Large particles with void spaces render them more susceptible to collapse during water uptake, hence the shrinking behavior.

To our knowledge, our studies here are the first to quantitatively explore the water uptake of aminophenols and their size-dependent growth factor under subsaturated conditions. Hence, our data add a new dimension to the growing hygroscopicity database of different OA with different functional groups and also highlight that importance of characterizing the physicochemical properties of OA to better explain their hygroscopicity, specifically bulk water solubility limits and morphological changes with water uptake. It should be noted that OA is generally found mixed with other atmospheric components, which could potentially lead to different hygroscopic properties. However, elucidating on the hygroscopic properties of pure OA provides significant insight on the properties that influence water uptake. Accordingly, our study emphasizes that to accurately predict the climate impact of OA, hygroscopicity and water uptake models need to be amended with aerosol physicochemical properties, such as chemical structure, solubility, and morphology. Our current work involves elucidating on the effect of mixing on the hygroscopicity of aromatic NOC.

Author contributions.

HAA conceived the idea with AAA And KAM. KAM designed, collected, and analyzed H-TDMA, and CCN experimental data. DR produced and analyzed TEM images. All authors contributed to the writing and preparation of the manuscript.

Supporting Information Available

Detailed experimental procedures, and figures and tables showing data analysis. This material is available free of charge on Environmental Science: Processes & Impacts.

ORCID

Akua Asa-Awuku: 0000-0002-0354-8368

Hind A. Al-Abadleh: 0000-0002-9425-0646

Kotiba A. Malek: 0000-0002-9326-3859

Dewansh Rastogi: 0000-0002-5416-0048

References

1　U. Pöschl, Atmospheric aerosols: composition, transformation, climate and health effects, *Angew. Chemie Int. Ed.*, 2005, **44**, 7520–7540.

2　M. C. Jacobson, H. C. Hansson, K. J. Noone and R. J. Charlson, Organic atmospheric aerosols: Review and state of the science, *Rev. Geophys.*, 2000, **38**, 267–294.

3　L. Chen, C. Peng, W. Gu, H. Fu, X. Jian, H. Zhang, G. Zhang, J. Zhu, X. Wang and M. Tang, On mineral dust aerosol hygroscopicity, *Atmos. Chem. Phys.*, 2020, **20**, 13611–13626.

4　S. M. Kreidenweis, M. Petters and U. Lohmann, 100 years of progress in cloud physics, aerosols, and aerosol chemistry research, *Meteorol. Monogr.*, 2019, **59**, 11.

5　S. Slikboer, L. Grandy, S. L. Blair, S. A. Nizkorodov, R. W. Smith and H. A. Al-Abadleh, Formation of Light Absorbing Soluble Secondary Organics and Insoluble

Polymeric Particles from the Dark Reaction of Catechol and Guaiacol with Fe(III), *Environ. Sci. Technol.*, 2015, **49**, 7793–7801.

6   B. Ervens, B. J. Turpin and R. J. Weber, Secondary organic aerosol formation in cloud droplets and aqueous particles (aqSOA): a review of laboratory, field and model studies, *Atmos. Chem. Phys.*, 2011, **11**, 11069–11102.

7   J. H. Seinfeld and S. N. Pandis, *Atmos. Chem. Phys.*, 2006, 5, 139–152.

8   J. Haywood and O. Boucher, Estimates of the direct and indirect radiative forcing due to tropospheric aerosols: A review, *Rev. Geophys.*, 2000, **38**, 513–543.

9   H. Yu, Y. J. Kaufman, M. Chin, G. Feingold, L. A. Remer, T. L. Anderson, Y. Balkanski, N. Bellouin, O. Boucher, S. Christopher, P. DeCola, R. Kahn, D. Koch, N. Loeb, M. S. Reddy, M. Schulz, T. Takemura and M. Zhou, A review of measurement-based assessments of the aerosol direct radiative effect and forcing, *Atmos. Chem. Phys.*, 2006, **6**, 613–666.

10   D. J. Jacob, J. M. Waldman, J. W. Munger and M. R. Hoffmann, in *Journal of Geophysical Research*, Cambridge University Press, 1986, vol. 91, pp. 1089–1096.

11   B. J. Murray, D. O'sullivan, J. D. Atkinson and M. E. Webb, Ice nucleation by particles immersed in supercooled cloud droplets, *Chem. Soc. Rev.*, 2012, **41**, 6519–6554.

12   N. Bellouin, J. Quaas, E. Gryspeerdt, S. Kinne, P. Stier, D. Watson-Parris, O. Boucher, K. S. Carslaw, M. Christensen and A. Daniau, Bounding global aerosol radiative forcing of climate change, *Rev. Geophys.*, 2020, **58**, e2019RG000660.

13   M. Kanakidou, J. H. Seinfeld, S. N. Pandis, I. Barnes, F. J. Dentener, M. C. Facchini, R. Van Dingenen, B. Ervens, A. Nenes, C. J. Nielsen, E. Swietlicki, J. P. Putaud, Y. Balkanski, S. Fuzzi, J. Horth, G. K. Moortgat, R. Winterhalter, C. E. L. Myhre, K. Tsigaridis, E. Vignati, E. G. Stephanou and J. Wilson, Organic aerosol and global climate modelling: A review, *Atmos. Chem. Phys.*, 2005, **5**, 1053–1123.

14   D. A. Knopf, P. A. Alpert and B. Wang, The Role of Organic Aerosol in Atmospheric Ice Nucleation: A Review, *ACS Earth Sp. Chem.*, 2018, **2**, 168–202.

15   A. Laskin, J. Laskin and S. A. Nizkorodov, Chemistry of atmospheric brown carbon, *Chem. Rev.*, 2015, **115**, 4335–4382.

16   M. Hallquist, J. C. Wenger, U. Baltensperger, Y. Rudich, D. Simpson, M. Claeys, J. Dommen, N. M. Donahue, C. George and A. H. Goldstein, The formation, properties and impact of secondary organic aerosol: current and emerging issues, *Atmos. Chem. Phys.*, 2009, **9**, 5155–5236.

17   J. H. Kroll and J. H. Seinfeld, Chemistry of secondary organic aerosol: Formation and evolution of low-volatility organics in the atmosphere, *Atmos. Environ.*, 2008, **42**, 3593–3624.

18   M. Mahilang, M. K. Deb and S. Pervez, Biogenic secondary organic aerosols: A review on formation mechanism, analytical challenges and environmental impacts, *Chemosphere*, 2021, **262**, 127771.

19   P. Liu, Y. J. Li, Y. Wang, A. P. Bateman, Y. Zhang, Z. Gong, A. K. Bertram and S. T. Martin, Highly viscous states affect the browning of atmospheric organic particulate matter, *ACS Cent. Sci.*, 2018, **4**, 207–215.

20   T. Moise, J. M. Flores and Y. Rudich, Optical Properties of Secondary Organic Aerosols and Their Changes by Chemical Processes, *Chem. Rev.*, 2015, **115**, 4400–4439.

21   M. A. Wedyan, K. G. Fandi and S. Al-Rousan, Bioavailability of atmospheric dissolved organic nitrogen in the marine aerosol over the Gulf of Aqaba, *Aust J Basic*, 2007, **1**, 208–212.

22   P. J. Milne and R. G. Zika, Amino acid nitrogen in atmospheric aerosols: Occurrence, sources and photochemical modification, *J. Atmos. Chem.*, 1993, **16**, 361–398.

23   Q. Zhang, C. Anastasio and M. Jimenez-Cruz, Water-soluble organic nitrogen in atmospheric fine particles (PM2. 5) from northern California, *J. Geophys. Res. Atmos.*, 2002, **107**, AAC-3.

24   S. Cornell, K. Mace, S. Coeppicus, R. Duce, B. Huebert, T. Jickells and L. Zhuang, Organic nitrogen in Hawaiian rain and aerosol, *J. Geophys. Res. Atmos.*, 2001, **106**, 7973–7983.

25   A. Laskin, J. S. Smith and J. Laskin, Molecular characterization of nitrogen-containing organic compounds in biomass burning aerosols using high-resolution mass spectrometry, *Environ. Sci. Technol.*, 2009, **43**, 3764–3771.

26   A. I. Darer, N. C. Cole-Filipiak, A. E. O'Connor and M. J. Elrod, Formation and stability of atmospherically relevant isoprene-derived organosulfates and organonitrates, *Environ. Sci. Technol.*, 2011, **45**, 1895–1902.

27   Y. Liu, J. Liggio, R. Staebler and S.-M. Li, Reactive uptake of ammonia to secondary organic aerosols: kinetics of organonitrogen formation, *Atmos. Chem. Phys.*, 2015, **15**, 13569–13584.

28   K. Vidović, D. Lašič Jurković, M. Šala, A. Kroflič and I. Grgić, Nighttime aqueous-phase formation of nitrocatechols in the atmospheric condensed phase, *Environ. Sci. Technol.*, 2018, **52**, 9722–9730.

29   G. Zhang, X. Lian, Y. Fu, Q. Lin, L. Li, W. Song, Z. Wang, M. Tang, D. Chen and X. Bi, High secondary formation of nitrogen-containing organics (NOCs) and its possible link to oxidized organics and ammonium, *Atmos. Chem. Phys.*, 2020, **20**, 1469–1481.

30   M. D. Petters and S. M. Kreidenweis, A single parameter representation of hygroscopic growth and cloud condensation nucleus activity, *Atmos. Chem.*

25

Phys., 2007, **7**, 1961–1971.

31   S. R. Suda and M. D. Petters, Accurate determination of aerosol activity coefficients at relative humidities up to 99% using the hygroscopicity tandem differential mobility analyzer technique, *Aerosol Sci. Technol.*, 2013, **47**, 991–1000.

32   A. Pajunoja, A. T. Lambe, J. Hakala, N. Rastak, M. J. Cummings, J. F. Brogan, L. Hao, M. Paramonov, J. Hong, N. L. Prisle, J. Malila, S. Romakkaniemi, K. E. J. Lehtinen, A. Laaksonen, M. Kulmala, P. Massoli, T. B. Onasch, N. M. Donahue, I. Riipinen, P. Davidovits, D. R. Worsnop, T. Petäjä and A. Virtanen, Adsorptive uptake of water by semisolid secondary organic aerosols, *Geophys. Res. Lett.*, 2015, **42**, 3063–3068.

33   A. Zuend and J. H. Seinfeld, Modeling the gas-particle partitioning of secondary organic aerosol: the importance of liquid-liquid phase separation, *Atmos. Chem. Phys.*, 2012, **12**, 3857–3882.

34   E.-J. E. Ott, E. C. Tackman and M. A. Freedman, Effects of Sucrose on Phase Transitions of Organic/Inorganic Aerosols, *ACS Earth Sp. Chem.*, 2020, **4**, 591–601.

35   M. D. Petters and S. M. Kreidenweis, A single parameter representation of hygroscopic growth and cloud condensation nucleus activity–Part 3: Including surfactant partitioning, *Atmos. Chem. Phys.*, 2013, **13**, 1081–1091.

36   R. Zhang, A. F. Khalizov, J. Pagels, D. Zhang, H. Xue and P. H. McMurry, Variability in morphology, hygroscopicity, and optical properties of soot aerosols during atmospheric processing, *Proc. Natl. Acad. Sci.*, 2008, **105**, 10291–10296.

37   A. Marsh, R. E. H. Miles, G. Rovelli, A. G. Cowling, L. Nandy, C. S. Dutcher and J. P. Reid, Influence of organic compound functionality on aerosol hygroscopicity: dicarboxylic acids, alkyl-substituents, sugars and amino acids, *Atmos. Chem. Phys.*, 2017, **17**, 5583–5599.

38   A. T. Lambe, T. B. Onasch, P. Massoli, D. R. Croasdale, J. P. Wright, A. T. Ahern, L. R. Williams, D. R. Worsnop, W. H. Brune and P. Davidovits, Laboratory studies of the chemical composition and cloud condensation nuclei (CCN) activity of secondary organic aerosol (SOA) and oxidized primary organic aerosol (OPOA), *Atmos. Chem. Phys.*, 2011, **11**, 8913–8928.

39   A. J. Prenni, M. D. Petters, S. M. Kreidenweis, P. J. DeMott and P. J. Ziemann, Cloud droplet activation of secondary organic aerosol, *J. Geophys. Res. Atmos.*, , DOI:10.1029/2006JD007963.

40   M. N. Chan, S. M. Kreidenweis and C. K. Chan, Measurements of the hygroscopic and deliquescence properties of organic compounds of different solubilities in water and their relationship with cloud condensation nuclei activities, *Environ. Sci. Technol.*, 2008, **42**, 3602–3608.

41   M. Kuwata, W. Shao, R. Lebouteiller and S. T. Martin, Classifying organic

materials by oxygen-to-carbon elemental ratio to predict the activation regime of Cloud Condensation Nuclei (CCN), *Atmos. Chem. Phys.*, 2013, **13**, 5309–5324.

42   S. R. Suda, M. D. Petters, G. K. Yeh, C. Strollo, A. Matsunaga, A. Faulhaber, P. J. Ziemann, A. J. Prenni, C. M. Carrico and R. C. Sullivan, Influence of functional groups on organic aerosol cloud condensation nucleus activity, *Environ. Sci. Technol.*, 2014, **48**, 10182–10190.

43   S. Han, J. Hong, Q. Luo, H. Xu, H. Tan, Q. Wang, J. Tao, Y. Zhou, L. Peng and Y. He, Hygroscopicity of organic compounds as a function of organic functionality, water solubility, molecular weight, and oxidation level, *Atmos. Chem. Phys.*, 2022, **22**, 3985–4004.

44   Q. Luo, J. Hong, H. Xu, S. Han, H. Tan, Q. Wang, J. Tao, N. Ma, Y. Cheng and H. Su, Hygroscopicity of amino acids and their effect on the water uptake of ammonium sulfate in the mixed aerosol particles, *Sci. Total Environ.*, 2020, **734**, 139318.

45   M. N. Chan, M. Y. Choi, N. L. Ng and C. K. Chan, Hygroscopicity of water-soluble organic compounds in atmospheric aerosols: Amino acids and biomass burning derived organic species, *Environ. Sci. Technol.*, 2005, **39**, 1555–1562.

46   J. Ruiz-Jiménez, S. Hautala, J. Parshintsev, T. Laitinen, K. Hartonen, T. Petäjä, M. Kulmala and M.-L. Riekkola, Aliphatic and aromatic amines in atmospheric aerosol particles: Comparison of three ionization techniques in liquid chromatography-mass spectrometry and method development, *Talanta*, 2012, **97**, 55–62.

47   X. Ge, A. S. Wexler and S. L. Clegg, Atmospheric amines–Part I. A review, *Atmos. Environ.*, 2011, **45**, 524–546.

48   L. Hildebrandt Ruiz, A. L. Paciga, K. M. Cerully, A. Nenes, N. M. Donahue and S. N. Pandis, Formation and aging of secondary organic aerosol from toluene: changes in chemical composition, volatility, and hygroscopicity, *Atmos. Chem. Phys.*, 2015, **15**, 8301–8313.

49   S. Nakao, C. Clark, P. Tang, K. Sato and D. Cocker Iii, Secondary organic aerosol formation from phenolic compounds in the absence of NO x, *Atmos. Chem. Phys.*, 2011, **11**, 10649–10660.

50   K. E. H. Hartz, J. E. Tischuk, M. N. Chan, C. K. Chan, N. M. Donahue and S. N. Pandis, Cloud condensation nuclei activation of limited solubility organic aerosol, *Atmos. Environ.*, 2006, **40**, 605–617.

51   J. Duplissy, M. Gysel, M. R. Alfarra, J. Dommen, A. Metzger, A. S. H. Prevot, E. Weingartner, A. Laaksonen, T. Raatikainen and N. Good, Cloud forming potential of secondary organic aerosol under near atmospheric conditions, *Geophys. Res. Lett.*

52   M. Frosch, M. Bilde, P. F. DeCarlo, Z. Jurányi, T. Tritscher, J. Dommen, N. M. Donahue, M. Gysel, E. Weingartner and U. Baltensperger, Relating cloud

condensation nuclei activity and oxidation level of α-pinene secondary organic aerosols, *J. Geophys. Res. Atmos.*

53   X. Tang, D. Price, E. Praske, D. N. Vu, K. Purvis-Roberts, P. J. Silva, D. R. Cocker and A. Asa-Awuku, Cloud condensation nuclei (CCN) activity of aliphatic amine secondary aerosol, *Atmos. Chem. Phys.*, 2014, **14**, 5959–5967.

54   C. Peng, M. N. Chan and C. K. Chan, The hygroscopic properties of dicarboxylic and multifunctional acids: Measurements and UNIFAC predictions, *Environ. Sci. Technol.*, 2001, **35**, 4495–4501.

55   T. M. Raymond and S. N. Pandis, Cloud activation of single-component organic aerosol particles, *J. Geophys. Res. Atmos.*, 2002, **107**, AAC-16.

56   J. N. Dawson, K. A. Malek, P. N. Razafindrambinina, T. M. Raymond, D. D. Dutcher, A. A. Asa-Awuku and M. A. Freedman, Direct Comparison of the Submicron Aerosol Hygroscopicity of Water-Soluble Sugars, *ACS Earth Sp. Chem.*, 2020, **4**, 2215–2226.

57   A. D. Estillore, A. P. S. Hettiyadura, Z. Qin, E. Leckrone, B. Wombacher, T. Humphry, E. A. Stone and V. H. Grassian, Water uptake and hygroscopic growth of organosulfate aerosol, *Environ. Sci. Technol.*, 2016, **50**, 4259–4268.

58   S. S. Petters, D. Pagonis, M. S. Claflin, E. J. T. Levin, M. D. Petters, P. J. Ziemann and S. M. Kreidenweis, Hygroscopicity of organic compounds as a function of carbon chain length and carboxyl, hydroperoxy, and carbonyl functional groups, *J. Phys. Chem. A*, 2017, **121**, 5164–5174.

59   C. N. Cruz and S. N. Pandis, A study of the ability of pure secondary organic aerosol to act as cloud condensation nuclei, *Atmos. Environ.*, 1997, **31**, 2205–2214.

60   M. B. Altaf, D. D. Dutcher, T. M. Raymond and M. A. Freedman, Effect of particle morphology on cloud condensation nuclei activity, *ACS Earth Sp. Chem.*, 2018, **2**, 634–639.

61   D. J. Rader and P. H. McMurry, Application of the tandem differential mobility analyzer to studies of droplet growth or evaporation, *J. Aerosol Sci.*, 1986, **17**, 771–787.

62   C. N. Cruz and S. N. Pandis, Deliquescence and hygroscopic growth of mixed inorganic - Organic atmospheric aerosol, *Environ. Sci. Technol.*, 2000, **34**, 4313–4319.

63   N. F. Taylor, D. R. Collins, C. W. Spencer, D. H. Lowenthal, B. Zielinska, V. Samburova and N. Kumar, Measurement of ambient aerosol hydration state at Great Smoky Mountains National Park in the southeastern United States, *Atmos. Chem. Phys.*, 2011, **11**, 12085–12107.

64   S. Lance, J. Medina, J. Smith and A. Nenes, Mapping the operation of the DMT continuous flow CCN counter, *Aerosol Sci. Technol.*, 2006, **40**, 242–254.

65   G. C. Roberts and A. Nenes, A continuous-flow streamwise thermal-gradient CCN chamber for atmospheric measurements, *Aerosol Sci. Technol.*, 2005, **39**, 206–221.

66   R. H. Moore, A. Nenes and J. Medina, Scanning mobility CCN analysis-A method for fast measurements of size-resolved CCN distributions and activation kinetics, *Aerosol Sci. Technol.*, 2010, **44**, 861–871.

67   A. Wiedensohler, An approximation of the bipolar charge distribution for particles in the submicron size range, *J. Aerosol Sci.*, 1988, **19**, 387–389.

68   D. Rose, S. S. Gunthe, E. Mikhailov, G. P. Frank, U. Dusek, M. O. Andreae and U. Pöschl, Calibration and measurement uncertainties of a continuous-flow cloud condensation nuclei counter (DMT-CCNC): CCN activation of ammonium sulfate and sodium chloride aerosol particles in theory and experiment, *Atmos. Chem. Phys.*, 2008, **8**, 1153–1179.

69   F. Mei, A. Setyan, Q. Zhang and J. Wang, CCN activity of organic aerosols observed downwind of urban emissions during CARES, *Atmos. Chem. Phys.*, 2013, **13**, 12155–12169.

70   M. Frosch, M. Bilde, A. Nenes, A. P. Praplan, Z. Jurányi, J. Dommen, M. Gysel, E. Weingartner and U. Baltensperger, CCN activity and volatility of β-caryophyllene secondary organic aerosol, *Atmos. Chem. Phys.*, 2013, **13**, 2283–2297.

71   C. Peng, K. A. Malek, D. Rastogi, Y. Zhang, W. Wang, X. Ding, A. A. Asa-Awuku, X. Wang and M. Tang, Hygroscopicity and cloud condensation nucleation activities of hydroxyalkylsulfonates, *Sci. Total Environ.*, 2022, **830**, 154767.

72   H. Köhler, The nucleus in and the growth of hygroscopic droplets, *Trans. Faraday Soc.*, 1936, **32**, 1152–1161.

73   J. V Niemi, S. Saarikoski, H. Tervahattu, T. Mäkelä, R. Hillamo, H. Vehkamäki, L. Sogacheva and M. Kulmala, Changes in background aerosol composition in Finland during polluted and clean periods studied by TEM/EDX individual particle analysis, *Atmos. Chem. Phys.*, 2006, **6**, 5049–5066.

74   J. Wang, J. E. Shilling, J. Liu, A. Zelenyuk, D. M. Bell, M. D. Petters, R. Thalman, F. Mei, R. A. Zaveri and G. Zheng, Cloud droplet activation of secondary organic aerosol is mainly controlled by molecular weight, not water solubility, *Atmos. Chem. Phys.*, 2019, **19**, 941–954.

75   M. Y. Choi and C. K. Chan, Continuous measurements of the water activities of aqueous droplets of water-soluble organic compounds, *J. Phys. Chem. A*, 2002, **106**, 4566–4572.

76   M. Bilde, A. A. Zardini, J. Hong, M. Tschiskale and E. Emanuelsson, in *AGU Fall Meeting Abstracts*, 2014, vol. 2014, pp. A21K-3178.

77   V. Varutbangkul, F. J. Brechtel, R. Bahreini, N. L. Ng, M. D. Keywood, J. H. Kroll, R. C. Flagan, J. H. Seinfeld, A. Lee and A. H. Goldstein, Hygroscopicity of

secondary organic aerosols formed by oxidation of cycloalkenes, monoterpenes, sesquiterpenes, and related compounds, *Atmos. Chem. Phys.*, 2006, **6**, 2367–2388.

78   S. M. Kreidenweis and A. Asa-Awuku, Aerosol hygroscopicity: Particle water content and its role in atmospheric processes.

79   M. Bilde, B. Svenningsson, J. Mønster and T. Rosenørn, Even− odd alternation of evaporation rates and vapor pressures of C3− C9 dicarboxylic acid aerosols, *Environ. Sci. Technol.*, 2003, **37**, 1371–1378.

80   J. Chen, W.-C. Lee, M. Itoh and M. Kuwata, A significant portion of water-soluble organic matter in fresh biomass burning particles does not contribute to hygroscopic growth: an application of polarity segregation by 1-Octanol–water partitioning method, *Environ. Sci. Technol.*, 2019, **53**, 10034–10042.

81   S. R. Suda, M. D. Petters, A. Matsunaga, R. C. Sullivan, P. J. Ziemann and S. M. Kreidenweis, Hygroscopicity frequency distributions of secondary organic aerosols, *J. Geophys. Res. Atmos.*

82   I. Riipinen, N. Rastak and S. N. Pandis, Connecting the solubility and CCN activation of complex organic aerosols: a theoretical study using solubility distributions, *Atmos. Chem. Phys.*, 2015, **15**, 6305–6322.

83   S. Nakao, Why would apparent κ linearly change with O/C? Assessing the role of volatility, solubility, and surface activity of organic aerosols, *Aerosol Sci. Technol.*, 2017, **51**, 1377–1388.

84   M. D. Petters and S. M. Kreidenweis, A single parameter representation of hygroscopic growth and cloud condensation nucleus activity–Part 2: Including solubility, *Atmos. Chem. Phys.*, 2008, **8**, 6273–6279.

85   K. A. Malek, K. Gohil, H. A. Al-Abadleh and A. A. Asa-Awuku, Hygroscopicity of polycatechol and polyguaiacol secondary organic aerosol in sub-and supersaturated water vapor environments, *Environ. Sci. Atmos.*

86   Y. Cheng, H. Su, T. Koop, E. Mikhailov and U. Pöschl, Size dependence of phase transitions in aerosol nanoparticles, *Nat. Commun.*, 2015, **6**, 1–7.

87   O. Laskina, H. S. Morris, J. R. Grandquist, Z. Qin, E. A. Stone, A. V Tivanski and V. H. Grassian, Size matters in the water uptake and hygroscopic growth of atmospherically relevant multicomponent aerosol particles, *J. Phys. Chem. A*, 2015, **119**, 4489–4497.

88   M. Mahish and D. Collins, Analysis of a multi-year record of size-resolved hygroscopicity measurements from a rural site in the US, *Aerosol Air Qual. Res.*, 2017, **17**, 1489–1500.

89   E. Mikhailov, S. Vlasenko, S. T. Martin, T. Koop and U. Pöschl, Amorphous and crystalline aerosol particles interacting with water vapor: conceptual framework and experimental evidence for restructuring, phase transitions and kinetic limitations, *Atmos. Chem. Phys.*, 2009, **9**, 9491–9522.

90 E. Mikhailov, S. Vlasenko, R. Niessner and U. Pöschl, Interaction of aerosol particles composed of protein and saltswith water vapor: hygroscopic growth and microstructural rearrangement, *Atmos. Chem. Phys.*, 2004, **4**, 323–350.

91 K. H. Leong, Morphological control of particles generated from the evaporation of solution droplets: experiment, *J. Aerosol Sci.*, 1987, **18**, 525–552.

92 K. H. Leong, Morphological control of particles generated from the evaporation of solution droplets: theoretical considerations, *J. Aerosol Sci.*, 1987, **18**, 511–524.

93 D. R. Lide, CRC Handbook of Chemistry and Physics, 2013-2014, *Handb. Chem. Phys.*

94 J. Sun, F. Wang, Y. Sui, Z. She, W. Zhai, C. Wang and Y. Deng, Effect of particle size on solubility, dissolution rate, and oral bioavailability: evaluation using coenzyme Q10 as naked nanocrystals, *Int. J. Nanomedicine*, 2012, **7**, 5733.

95 K. R. Chu, E. Lee, S. H. Jeong and E.-S. Park, Effect of particle size on the dissolution behaviors of poorly water-soluble drugs, *Arch. Pharm. Res.*, 2012, **35**, 1187–1195.

1
2
3
4
5
6
7
8
9
10
11
12
13
14
15
16
17
18
19
20
21
22
23
24
25
26
27
28
29
30
31
32
33
34
35
36
37
38
39
40
41
42
43
44
45
46
47
48
49
50
51
52
53
54
55
56
57
58
59
60

31